Local Dynamic Frequency Response Using Domestic Electric Vehicles

Mazin T. Muhssin[a,b], Zeyad A. Obaid[c], Kassim Al-Anbarri[b], Liana M Cipcigan[a], Mazin N. Ajaweed[d]

[a]Institute of Energy, School of Engineering, Cardiff University, Cardiff, CF24 3AA, United Kingdom
[b]College of Engineering, Mustansiriyah University, Baghdad, Iraq
[c]College of Engineering, University of Diyala, Baqouba, Iraq
[d]Control and Systems Engineering, University of Technology, Baghdad, Iraq

Abstract There is an increasing interest to penetrate low carbon vehicles into the transport system. Take the Great Britain (GB) as an example, the number of electric and plug-in hybrid vehicles will make up to at least half of new vehicle sales. Electric vehicles (EVs) are expected to contribute to the ancillary services of the frequency response because EVs can provide immediate frequency response and sustain its response for considerable period of time. This paper addresses the design of a Dynamic Vehicle Grid Support (DVGS) control algorithm for the provision of local frequency response. The DVGS considers a dynamic relationship between the state of charge of EVs and frequency set-points. Thus, it can be installed locally avoiding the cost and the time delay associated with the communication system between EVs and the control centre. The DVGS control algorithm was demonstrated using the reduced GB transmission power system model with a reduced system inertia. The simulation results showed that the EVs are promising assets for the provision of frequency response and reducing the rate of change of frequency (RoCoF). Moreover, EVs can be controlled geographically to provide the zonal frequency response, reducing the dependency on the power from the spinning reserve, especially with a reduced system inertia. The financial benefits of using the aggregated DVGS for firm frequency response (FFR) service in the GB is calculated.

1. Introduction

The generation and consumption sectors of the modernized power systems are undergoing significant changes. The increasing levels of the intermittent generation sources provide a fluctuating output which can impact the mismatch of power between the generation and the supply. In addition, the use of electric vehicles (EVs) with uncontrolled charging schemes and the electrification of heat systems can result in a higher power mismatch. Therefore, the electrical power system requires new capabilities and control schemes to maintain the fundamental levels of reliability, including frequency and voltage response [1-4]. The new frequency control measures are provided by three main elements generation, demand, and storage systems. However, the focus of the literature review for this paper is on the demand and storage elements for the provision of the frequency response.

1.1 Relevant Work

Recently, considerable attention has been paid to residential and industrial flexible assets, where the topic of demand response has been addressed in several scientific publications. The Thermostatically Controlled Load (TCL) units were used as flexible loads to balance the power of generation with demand [5-9]. For example,

in [5, 6], the researchers studied the usage of industrial loads as sources of ancillary services, while references [7-9] investigated the usage of household appliances, such as refrigerators and heat pumps, to regulate the grid frequency with a high renewable energy penetration. Because of the thermal storage characteristics, the normal operation of these assets was temporarily interrupted to mitigate a severe frequency deviation without undermining the temperature. In [6, 7], a dynamic frequency control algorithm (DFC) was developed to reduce the power consumption of domestic heat pumps and industrial bitumen tanks in response to a loss of a generation unit. The DFC algorithm used a dynamic relationship between the temperature and the pre-defined trigger frequencies to switch off the loads smoothly and to avoid a severe load payback after the frequency recovery.

The participation of demand in the frequency response markets was investigated in [9, 10]. In [10], the researchers introduced an innovative market structure, where the 'mean field game' method was used to coordinate the complex interactions of groups of TCL units and the grid. In [9], different TCL assets were combined to provide a Firm Frequency Response (FFR) service.

Several publications have addressed the role of storage systems in the development of the future electric grid. In [11-13], various storage technologies for grid support were reviewed and the importance of storage systems for energy delivery was presented. References [14, 15] have proposed simplified models to integrate a number of small-size energy storage units, including batteries and flywheels, into the grid. In [16, 17], hierarchal control for a battery population using a Markov chain was developed to mimic the frequency deviation. It was concluded that a population of small-size storage systems could provide a frequency response similar to the response obtained from the generation units.

In recent years, there has been an increasing interest in EVs from the environmental, technical, and economic perspectives. For example, Element Energy, an energy consultancy in the UK, carried out a comprehensive study to assess the potential effects of EVs on the power system from the abovementioned perspectives [18].

Typically, the residential EVs are available for charging for 8 to 11 hours per day, but only need 3 to 7 hours for full charging depending on the charging scheme [18]. Therefore, the charging of EVs can be interrupted on the basis of a signal from the operator for a certain period of time without undermining the charging function. In [19], a tool was proposed to estimate three types of EV charging strategies (dumb, off-peak, and smart charging). The EVs were used to provide the primary frequency response for the Great Britain (GB) power system. In [20], a smart charging strategy for of EVs was presented to mitigate the effect of the fluctuation of the renewable energy sources (RES) outputs.

In parallel, other researchers have proposed a dynamic frequency control strategy for EVs, taking into account the travelling behaviour of the EV users. In addition, the droop control method was used to regulate the EV charging power, offering a frequency response with the presence of high levels of renewables. It has been concluded that the controlled response drawn by EVs can be the same as the response of the generating units [21, 22]. In this study, we have developed a new frequency control algorithm. Instead of using the droop control method, a low and high frequency set-points were used and are dynamically updated with the state of charge of EVs throughout the time. Also, a new control algorithm during critical time was presented to ensure that each EV reached fully charge by the morning.

1.2 Contribution of This Study

The design of a suitable control algorithm for the provision of the frequency response from EVs is yet under development. In this study, we investigated the effects of aggregated EVs on the grid frequency. A dynamic frequency control algorithm was developed to disconnect the charging of EVs in response to an operator's signal. The control algorithm presented in this paper is hereafter named Dynamic Vehicle Grid Support (DVGS). The frequency control algorithms for EVs have been previously applied in the application of power systems [21-23]. The main novelties of this paper to the state of art are firstly, to adopt a dynamic relationship between the state of charge of each individual EV and grid frequency set-points assigned to each EV. The frequency set points are updated continuously (and dynamically) based on the state of charge of EVs. Secondly, to use a new way to control the charging process during the critical time to ensure that the user will receive his/her EV fully charged in the morning regardless the frequency event. The control algorithm in this paper provides many advantages: 1) it can be installed locally near to the charging point. Thus, avoiding the cost and the time delay associated with the communication system with the control center, 2) provide smooth frequency response as the population of EVs will be tripped gradually based on the dynamic relationship between the frequency set-points and the EVs' state of charge, and 3) at the end, every EV is fully charged. The following aspects are considered throughout this study:

- It seems that several of research studies that have been done on the vehicle-to-grid (V2G) technology (in population) were optimistic in terms of economic viability, impact on battery, and social acceptance. However, the design of the DVGS aims to control the behavior of the charging EVs without performing vehicle-to-grid (V2G) technology. This could provide another view for the capability of EVs to provide frequency response.

- A dynamic relationship is adopted through the design of the DVGS controller so that the frequency set-points vary dynamically with the state of charge of the EVs.

- The whole control algorithm is developed to shape the system operator's understanding about the potential role of residential EVs to provide frequency response and reducing the rate of change of frequency (RoCoF). This was done by examining the capability of DVGS control algorithm to provide dynamic frequency response to the reduced GB transmission power system model through a collaborative work with National Grid.

- The frequency control algorithm does not interfere with the normal operation of the charging process, i.e. every individual EV will be fully charged at the end. This was done by accessing the DVGS with a charging control algorithm during critical time.

- The financial benefits of the aggregated EVs to participate in the balancing service based on the present operational practice of the GB power system is investigated.

2 Generic Model of EV Charger

Fig. 1 shows the generic EV charging system [19, 24]. The generic model has a DC–DC converter to step down the voltage for the EV charger. The model also contains an inverter connected to the grid. The resistor

represents the resistance of the reactor and the inverter losses. The inverter is controlled using a pulse-width modulation (PWM) switching technique. Active and reactive power controls were used with vector control, which was utilised to provide the modulating signals for PWM.

The current $i(t)$ in Fig. 1 was governed by a first-order differential equation as shown in (1).

$$L\frac{di(t)}{dt} + Ri(t) + V_{EV} = V_{grid} \tag{1}$$

However, the voltage between the EV terminals V_{EV} can be written as in (2), where the value of the constant α (0.5 or 1.0) depends on the topology of the inverter. M is the PWM modulation index of the inverter, w is the angular velocity of the grid, and δ is the angle between the voltage of the grid and V_{EV} [24].

$$V_{EV} = \alpha M V_{DC} \sin(wt + \delta) \tag{2}$$
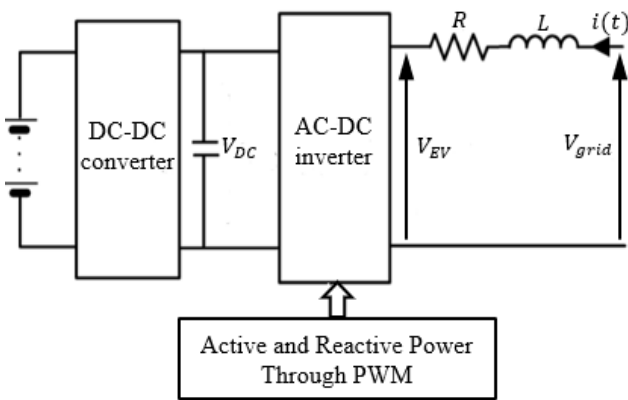
Fig. 1 The generic EV charging system
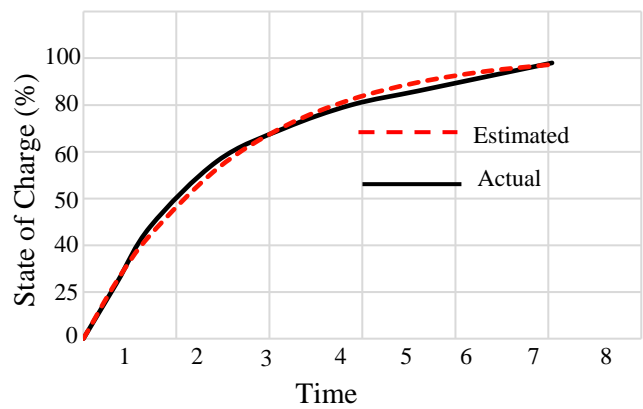
Fig. 2 Charging profile for lead acid battery

3   Configuration of Electric Vehicles

Electric vehicles have different types of battery systems, but the lead-acid and Li-ion batteries are the most relevant technologies [25, 26]. This study considered the use of the lead-acid battery technology for domestic EVs. Moreover, the study considered only the slow charging process as this is the most common way to charge EVs at home [18]. Thus, the rated power of 3 kW for home charging, typical in the UK is considered. A simplified curve fitting method was used to model the behaviour of the EV charging based on an actual charging profile given in [19]. Equation (3) was used to fit the behaviour of the actual state of charge SoC of the EVs, where μ is the coefficient of the nominal zone, σ is the coefficient of the exponential zone, and ɳ is the charging time constant. Fig. 2 shows the actual and the estimated SoC profile, using (3), for an EV with a lead-acid battery. According to [25, 26], the speed of charging the lead acid battery is quicker when its SoC is low and slower when its SoC is higher. This can be also shown in Fig. 2, for example, at time 0-2 hours, the SoC has increased by 50% (from 0% to 50%) while between 4-6 hours, the SoC has increased by approximately 20% (from 75% to 95%). Every EV requires approximately 5 hours, (if its initial SoC is 50%) and 3 hours (if its initial SoC is 75%) for full charging. Hence, the EVs can participate in the ancillary services of the frequency response by disconnecting their charging process whenever they are available for charging.

$$SOC(\mu, \sigma, \eta) = \mu + \sigma e^{-t/\eta} \tag{3}$$

4 The Design of DVGS Control Algorithm

The components of the DVGS control algorithm are shown in Fig. 3. The whole control system is setup locally next to the charging point. The DVGS is equipped with a frequency sensor to measure the grid frequency locally. It is also equipped with a clock to measure the time of day. The user inputs (such as desired SoC and the time that which charging required to be completed) can be managed locally within the internal control unit (or may be specified remotely). It is assumed that the population of EVs driven by decentralised DVGS units will be distributed widely among the network where the volume of the dynamic frequency response can be predicted based on the number of charging units, hence, the unnecessarily centralized control with the third party which results in significant time delay can be avoided. However, the third party (such as an aggregator or National Grid) can still communicate with the control unit to monitor the power consumption. This assumption was also adopted by several studies [6, 18].

 The control algorithm of the DVGS, outlined in Fig. 3, is divided into three blocks: Blocks A, B and C.

4.1 Charging Control Algorithm

This part is shown in Block A of Fig. 3. The Charging Control algorithm is responsible for controlling the charging state of the EV's battery on the basis of the status of the EV's SoC. The Charging Control algorithm measures the SoC of the EV's battery and generates the charging state signal S_{ch}^{ev}. The Charging Controller turns the S_{ch}^{ev} signal to '1' to charge the EV's battery and to '0' to disconnect the charging. The power consumption of a group of EVs can be represented by (4). P_{chr} is the charging power consumed by the EVs' batteries during the normal charging period. P_{ev} is the kilowatt power of an EV battery. NEV is the number of EVs.

 The algorithm of the Charging Controller is explained in Table 1 (rows 1 and 2). As shown in row 1, if the SoC of an EV is lower than 10%, the charging process is prioritised irrespective of the frequency incidents. In this case, the Charging Controller turns the S_{ch}^{ev} signal to '1', and the power consumption of the vehicles P_{con} (shown in Fig. 3) is set to P_{chr} based on (4).

However, if an EV reaches the maximum charging value (as shown in row 2), the Charging Controller disconnects the charging process by setting the S_{ch}^{ev} signal to '0', and hence, P_{con} becomes 0 kW.

$$P_{chr} = \sum_{k=1}^{NEV} S_{ch}^{ev} \times P_{ev} \qquad 0\% \leq SOC \leq 90\% \tag{4}$$

$$P_{VGS} = \sum_{k=1}^{NEV} S_{VGC-1,2}^{ev} \times P_{ev} \qquad 10\% \leq SOC \leq 90\% \tag{5}$$
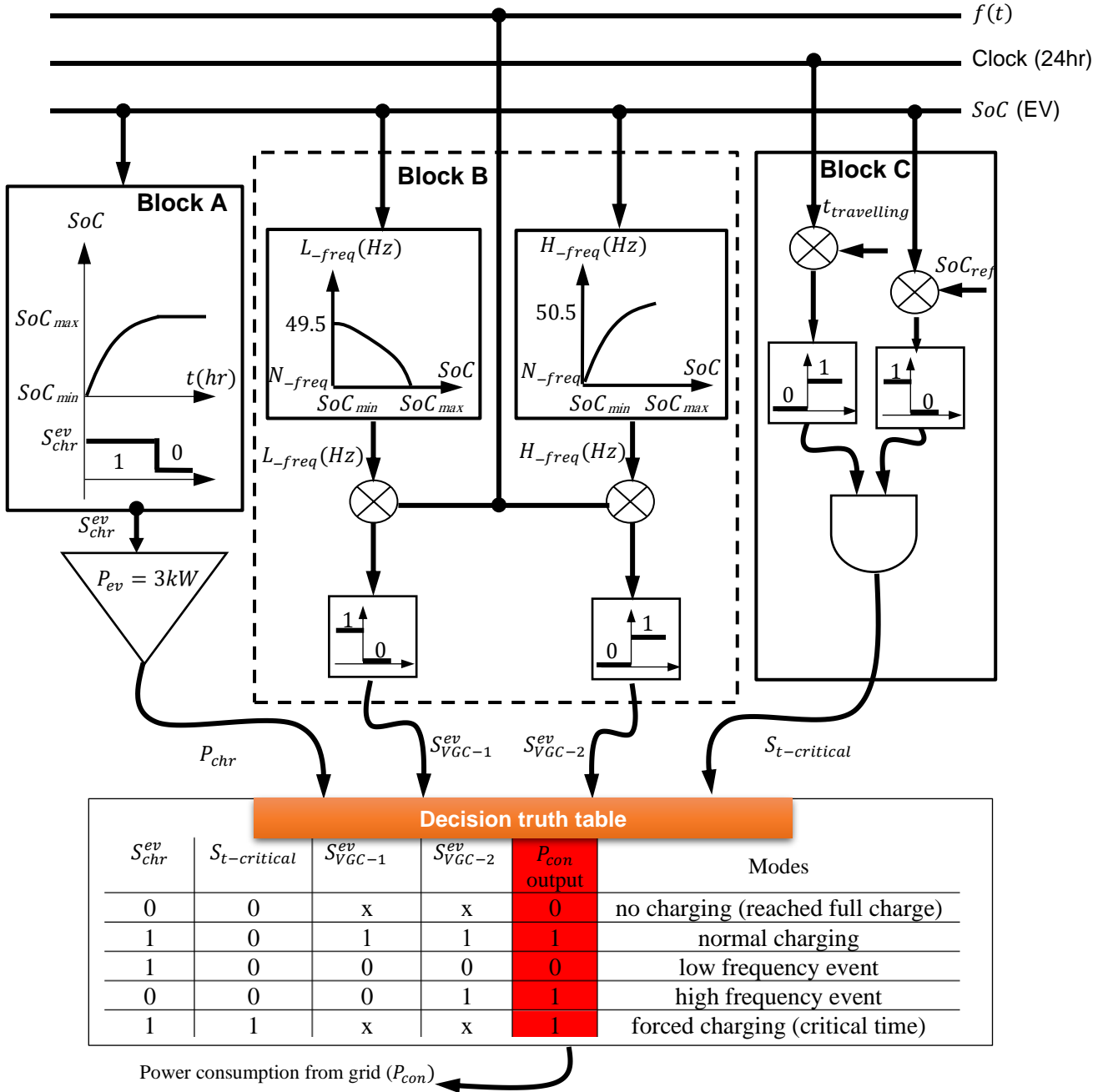
Fig. 3 Framework of EV frequency control system (DVGS controller)

4.2 Frequency Control Algorithm

This part is shown in Block B of Fig. 3. The second part of the control algorithm is the Frequency Control algorithm, which aims to control the grid frequency by disconnecting the charging EVs on the basis of a frequency signal. The power consumption of a group of EVs can be represented by (5). P_{VGS} is the curtailed power obtained by disconnecting the charging EVs during the occurrence of the frequency event. S_{VGS}^{ev} is the control state signal which controls the charging state of the EVs from the frequency control side. For instance, the Frequency Controller sets $S_{VGS,1}^{ev}$ to '0' to disconnect the charging when there is a low-frequency event and $S_{VGS,2}^{ev}$ to '1' for the occurrence of a high-frequency event.

As shown in Block B of Fig. 3, the frequency controller of each EV was assigned with two frequency set-points, namely the low- and the high-frequency set-points (L_{-freq} and H_{-freq}, respectively). The threshold

of these set-points can be adjusted by the operator according to the GB grid code for delivering the service [7]. However, the ranges $(-0.015\,Hz, -0.5\,Hz)$ and $(0.015\,Hz, 0.5\,Hz)$ were assigned to the L_{-freq} and H_{-freq} set-points. The ranges of these set-points were chosen to conform to lower and upper threshold of the dynamic FFR service of National Grid with deadband equal to $\pm 0.015Hz$ [1].

The Frequency controller compares the grid frequency $f(t)$ with the frequency set-points to check for the frequency change incidents. As shown in Table 1 (rows 3–5), when the grid frequency $f(t)$ drops lower than L_{-freq} this implies that there is a low-frequency incident. To maintain the health of the EV's battery, the low frequency controller is only activated when SoC is greater than 10% The frequency controller then sets P_{con} to P_{VGC} and $S_{VGS,1}^{ev}$ to '0' on the basis of (5) to disconnect the responsive EVs and reduce the power consumption of the EVs. Similarly, if grid frequency increases to more than H_{-freq} (as shown in row 5), this means that there is a high-frequency incident. The frequency controller then drives the EVs to the charging mode (i.e., $P_{con} = P_{VGS}$ and $S_{VGS,2}^{ev} = 1$) to increase the power consumption. As shown in row 5, if the grid frequency $f(t)$ has a value between L_{-freq} and H_{-freq} and also if the SoC lies in the range $[0\% - 90\%]$, this means that there is no frequency event and the normal operation of the charging system has to be maintained. Therefore, the frequency controller sets S_{VGS}^{ev} to '1' and P_{con} to P_{VGC} on the basis of (5).

Then, the all signals (P_{chr}, $S_{VGC-1,2}^{ev}$, and $S_{t-critical}$) were connected to logic gates to obtain the final power consumption from the grid according to the descion truth table shown in Fig. 3. Delay of a minimum 1min was given to avoid frequent charging/stop charging actions which may affect the battery life.

Table 1 Frequency Control Algorithm

	CONDITIONS	**CHARGING CONTROLLER**	**FREQUENCY CONTROLLER**
row1	$Soc \leq 10\%$	$S_{Ch}^{ev}=1$ $P_{con} = P_{chr}$ Based on (4)	−
row2	$Soc \geq 90\%$	$S_{Ch}^{ev}=0$ $P_{con} = 0$ Based on (4)	−
row3	$f(t) \leq L_{-freq}$ AND $10\% \leq SoC \leq 90\%$	−	$S_{VGS-1}^{ev}=0$ $P_{con} = P_{VGS}$ Based on (5)
row4	$f(t) \geq H_{-freq}$ AND $10\% \leq Soc \leq 90\%$	−	$S_{VGS-2}^{ev}=1$ $P_{con} = P_{VGC}$ Based on (5)
row5	$L_{-freq} \leq f(t) \leq H_{-freq}$ $0\% \leq Soc \leq 90\%$	−	$S_{VGS}^{ev}=1$ $P_{con} = P_{VGC}$ Based on (5)

4.3 *Dynamic Relationship between SoC and Frequency Set-points*

In this study, the frequency set-points (L_{-freq} and H_{-freq}) were chosen to vary dynamically with the SoC of the EVs according to the 2nd degree polynomial dynamic shape presented in Fig. 4. The 2nd degree

polynomial shape was used instead of the linear shape to expand the region of the triggering action which causes more EVs to respond quicker to the frequency event. Hence, the whole control algorithm was named the Dynamic Vehicle Grid Support (DVGS) control algorithm. The threshold of these set-points can be adjusted by the operator according to the GB grid code for delivering the service [7]. However, the ranges $(-0.015 \text{ Hz}, -0.5 \text{ Hz})$ and $(0.015 \text{ Hz}, 0.5 \text{ Hz})$ were assigned to the L_{freq} and H_{freq} set-points. The ranges of these set-points were chosen to conform to lower and upper threshold of the dynamic FFR service of National Grid with deadband equal to ±0.015Hz.

Equations (6) and (7) were used to generate the 2nd degree polynomial shape in Fig. 4, where N_{-freq} is the nominal frequency with deadband = ±0.015 Hz. SoC_{min} and SoC_{max} are the minimum and the maximum SoC of the EVs. The main reasons to consider this dynamic relationship is: I) to make the frequency controller works independently from the system operator because the state of charge will be controlled dynamically against the frequency set-points at a local level. Thus, the operator does not need to monitor the state of charge of each individual EV in real time and the delay and the cost resulted from the communication system with the operator is avoided. II) to ensure a gradual disconnection and reconnection of the EVs in response to the grid frequency, avoiding load payback that would results from recharging large number of EVs simultaneously after the frequency event , and to prevent the unnecessary charging disconnections. This is performed as follows:

- If the frequency drops to lower than N_{-freq}, the dynamic relationship in (6) assigns a frequency set-point near to the EV that has SoC_{max}. Then, with the dynamic shape in Fig. 4(a), the EVs will have a gradual disconnection starting from SoC_{max} and in the descending order toward SoC_{min}. Thus, the charging EVs with a low SoC level, has less chances to be disconnected when there is a low-frequency event.

- If the frequency increases to more than N_{-freq}, the dynamic relationship in (7) assigns a frequency set-point near to the EV that has SoC_{min}. After, with the dynamic shape in Fig. 4(b), the EVs will be connected gradually to the charging mode starting from SoC_{min} and in the ascending order toward SoC_{max}.

$$L_{\_freq} = \frac{N_{-freq}-49.5}{(SoC_{max}-SoC_{min})^2}(SoC - SoC_{min})^2 + 49.5 \tag{6}$$

$$H_{\_freq} = \frac{50.5-N_{\_freq}}{(SoC_{max}-SoC_{\min})^2}(SoC - SoC_{min})^2 + N_{\_freq} \tag{7}$$
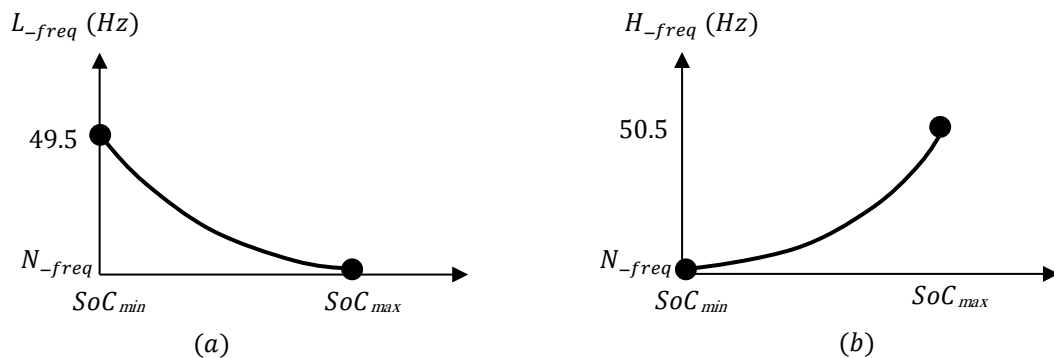
Fig.4 10 Dynamic relationship between the frequency set-points and the SoC (a) $L_{\_freq}$ set point (b) $H_{\_freq}$ set-point.

For the simulation of the DVGS Control algorithms, the following assumptions were considered for the operation of the charging process:

- The analysis of this study depends on the number of domestic EVs that can participate in the ancillary service of the frequency response only when they are plugged in to the charging. Based on the data provided in [18], domestic EVs are usually plugged in to the frequency control unit just when they come back home from work (between 17:00-21:00 should be charged by 06:00). At this stage, it is very complex to estimate how many EVs can participate in the dynamic frequency response for the rest time of day.

- The EVs' batteries usually come with an initial SoC level before they are plugged into the charger. Thus, the initial charging states of the EVs were randomised between 10% to 90% by using a uniform distribution.
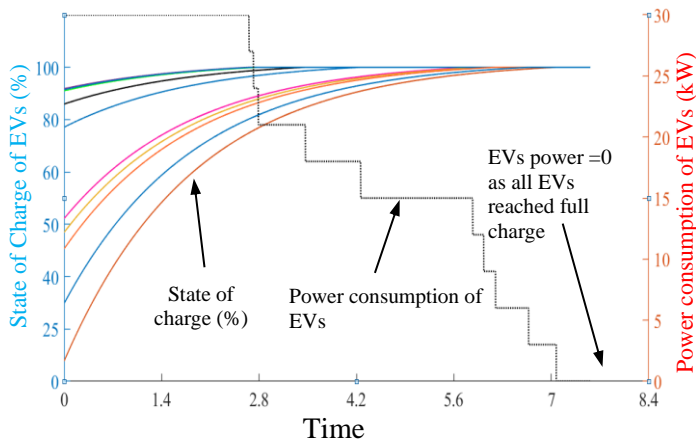
Fig.5 10 residential EVs being charged and their power consumption without frequency event
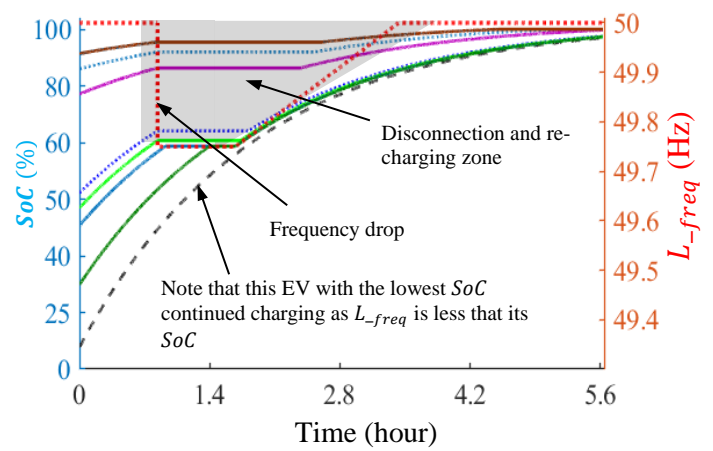
Fig.6 the charging of 10 residential EVs being controlled according to (6) and (7) against a frequency signal

The simulation results in Figs. 5 and 6 were presented to investigate the effect of the dynamic relationship between the EVs' $SoCs$ and the frequency set-points on the charging process with the presence of frequency drop. Fig. 5 shows the charging behaviour of 10 aggregated EVs being plugged into the charging point (left Y-axis). Fig. 5 also shows that the power consumption of the aggregated EVs has dropped to almost the minimum when the EVs are disconnected (right Y-axis). The frequency input signal $f(t)$ was set to a nominal value (i.e., 50 Hz), indicating a 'no frequency' event. At the beginning, the aggregated EVs consumed a maximum power, as all the EVs were charging at the same time. The aggregated power decreased gradually as the EVs' $SoCs$ converged to 100%. This was because the Charging Controller disconnected the charging process each time the battery reached full charge. When all the 10 EVs reached full charge, the power consumption approaches to zero, indicating that the charging process of the all the EVs ended.

In Fig. 6, a made of test frequency signal (right Y-axis, dotted red profile) was inserted into the model to examine the operation of the DVGS controller with the presence of the dynamic relationship given in (6) and (7). The frequency profile was given a step drop at $t = 0.83$ hour and a ramp recovery, started from $t = 1.66$ hour. We can observe that the 10 EVs were charging (Left Y-axis) until the frequency signal dropped suddenly to around 49.78 Hz. After the frequency drop, the charging process of nine EVs stopped gradually in descending order starting from the highest to lowest SoC. This was because the frequency set-points L_{-freq} exceeded the SoC levels of nine EVs ($L_{-freq} > SoC$). However, one EV (dashed black curve), which has the

lowest SoC level, continued its charging process until the end. This EV continued its charging process because of the dynamic relationship given in (6), where the frequency set-point L_{-freq} did not exceed the SoC of this EV $L_{-freq} < SoC$. After the frequency recovered at $t = 1.66$ hour, the nine EVs started to recharge again in the ascending order from the lowest to the highest SoC. The gradual recharging was based on (7), where each EV started to recharge each time its SoC value became higher than the L_{-freq} set-point. This dynamic behaviour between the SoC and the frequency set-points can be achieved locally in real time, thuse, avoiding the two communication ways with the system operator.

4.4 DVGS during the critical time

The algorithm of the charging controller during the critical time (shown in Block C of Fig. 3) was added to the DVGS to ensure that the user will receive his/her EV fully charged in the morning regardless the frequency event. This was done by measuring the critical time according to the SoC of each EV during the night. The critical time $t_{critical}$ is defined as the remaining time for charging the EV to get fully charged by the morning (before the travelling time). The $t_{critical}$ is calculated by using (8), where $t_{travelling}$ is the travelling time in the morning, $t_{current}$ is the current time of the day, and $SoC_{critical}$ is the critical state of charge of the EV. According to (8), the curve between the $t_{critical}$ and SoC is obtained and is shown in Fig. (7).

$$t_{critical} = [t_{travelling} - t_{current}] \; if \; (SoC \leq SoC_{critical})$$

(8)

The control algorithm (in Block C of Fig. 3) measures both the $t_{critical}$ and SoC and generates the critical-charging signal $S_{t-critical}$. If SoC is greater than the $SoC_{critical}$, the $S_{t-critical}$ is turned to '0' indicating a no critical-charging is required. Then, the DVGS will activate one of the other modes stated in the decision truth operation shown in Fig.3 (no charging, normal operation, low frequency event, or high frequency event). However, if SoC is less than the $SoC_{critical}$ at $t = t_{critical}$, the $S_{t-critical}$ is turned to '1' and P_{con} to '1' indicating a critical-charging (forced-charging) without any interrupting even if there is frequency incidents. For example, the charging behavior of two EVs (with random initial SoC) were simulated with the presence of DVGS algorithm before and after injecting a frequency event as shown in Fig. (8). Between times (22:00-22:40), both EVs were charging based on 'normal charging mode'. A Sudden drop of system frequency (around 49.4Hz) was injected at time 22:40 and hence the charging of both EVs were disconnected according to 'low frequency response' mode. However, EV_1 has reached the critical time $t_{critical}$ at Point A and therefore the DVGS sets EV_1 to 'critical charging' mode until it reached fully charge by 5:00 in the morning. At Point B, EV_2 has reached its critical time late at point B and was turned to 'critical charging' mode. In this way, all EVs were guaranteed to reach full charge before the travelling time.
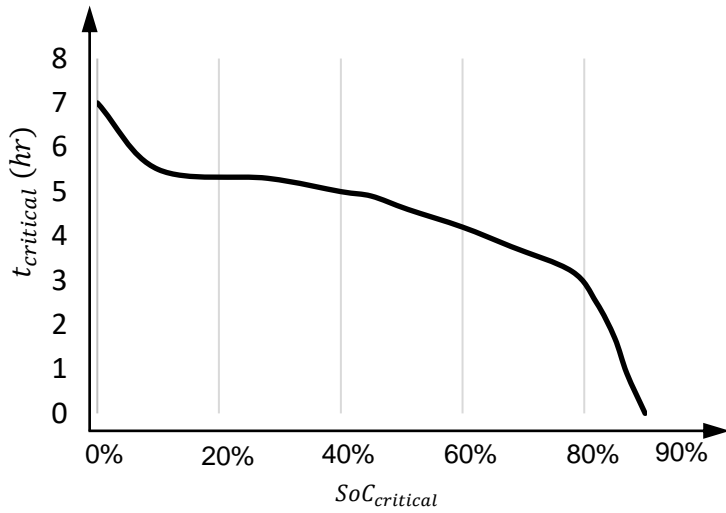
Fig.7 relationship between the $t_{critical}$ and SoC
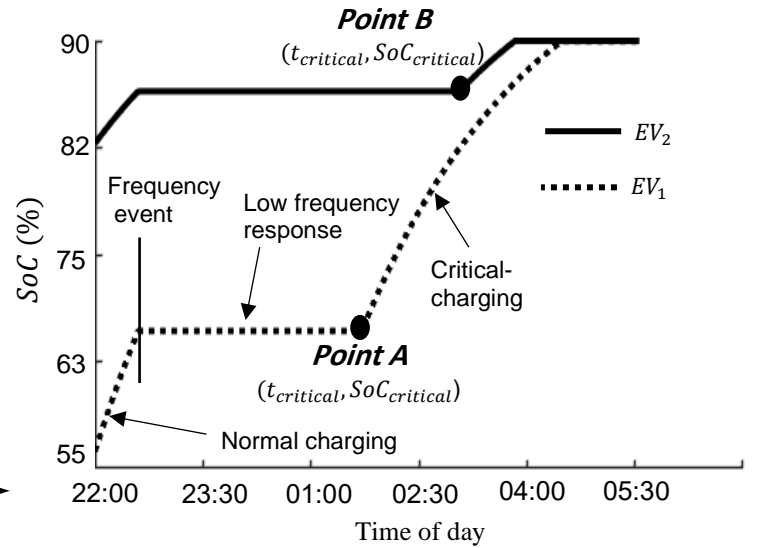
Fig.8 Charging behavior of two EVs with respect to low frequency event and critical time

5   Case Studies on the Reduced GB Dynamic Power System

5.1   Case Study 1

This case study was conducted through a collaborative work with National Grid. The reduced GB transmission power system model was used to assess the capability of the DVGS to provide a frequency response to a multi-geographical power system at the national level. This power system was modelled in PowerFactory by National Grid and was dispatched according to the National Grid Gone Green 2030 Future Energy Scenario. The schematic representation of this model is shown in Fig. 9 [27]; it consists of a 36-bus equivalent network representing the National Electricity Transmission System of the GB system. Each geographic zone in the model represents the synchronous and static generation units categorised according to the fuel types, demand, and HVDC interconnectors. The GB system inertia is predicted to reduce by around 70% by 2035 as compared to the 2014 levels. Therefore, the inertia constant of the synchronous generation units was reduced to 3sec with the system demand equal to 39 GW.

Aggregated EV models were connected to the 11 zones of the reduced GB model as a close geographical reflection to the GB Distribution Network Operators. The number of available EVs at each time of the day for the provision of a low-frequency response was estimated by Element Energy for the 2030 medium uptake scenario in the Great Britain [18] and was used as an input to the DVGS control algorithm. The aggregated total number of responsive EVs was distributed over the 11 zones according to the number of households in each zone [28], as shown in Table 2. A 1724-MW generator unit located in zone 23 was tripped at $t =$ 5sec, which represents the level of power infeed risk in the GB power system [7].

Fig. 10 shows the power consumption of the EVs in 11 zones after the use of the DVGS controller. It can be seen that the EVs provided an immediate zonal frequency response (once the frequency dropped lower than the deadband = 49.985 Hz) in proportion to the frequency drop at $t = 5$sec. The total frequency response drawn by the aggregated EVs in the different zones was 650 MW. After the frequency recovery, we can see that the charging power is recovered smoothly avoiding the load payback that would result from large number of EVs start recharging at the same time.

Fig. 11 shows the grid frequency with and without the use of the DVGS controller. We observed that the DVGS controllers of 300k aggregated EVs reduced the frequency deviation from 49.1Hz to 49.57Hz within only 8sec and maintained the frequency within the threshold limit defined by National Grid, i.e. $\leq 49.5\ Hz$.

Fig. 12 shows the total change of the aggregated power output from six nuclear, two gas, one hydro, one biomass, and one pump storage generators located in different zones in the reduced GB power system. As can be seen, the generation power exhibited a significant reduction after the use of the DVGS controller.

Fig. 13 shows the total reduction of the charging power after the frequency event. Around 650MW was reduced to recover the frequency, which account for 216k responsive EVs. However, there still 84k EVs were not responded to the frequency event because they were either reached fully charge before the frequency event or their frequency set- points were less than the grid frequency. V2G technology is important to control the behavior of the fully charged EVs in response to the grid frequency. However, comprehensive studies are required to address its technical benefits in comparison to the economic viability, impact on battery, and social acceptance.

In conclusion, the DVGS control algorithm of EVs could sustain its frequency response for several hours depending on the level of the SoC and the time of the frequency incident. This was attributed to the fact that the population of EVs has different $SoCs$ levels and that they do not require a long time to reach full charge after the recovery of the grid frequency. The frequency response obtained from the EVs allowed the grid frequency to be recovered by using stand-by generation units, responding after hours, rather than using the power from the expensive spinning reserve responding in real time.

Table 2 Number of EVs in Each Zone

Zones number	Location of Zones	No. EVs at times 18:00-21:00
Zone-32	North Scotland	13950
Zone-27W	Central and Southern	17680
Zone-18	North East England	26500
Zone-26	North West England	26500
Zone-14A	Yorkshire	26500
Zone-19	East England	28233
Zone-15	London	28233
Zone-10	South East England	28233
Zone-2	Southern England	24000
Zone-9	Merseyside, Chershire, North Wales, North Shropshire	19000
Zone-13	E. Midlands, W..Midlands, S. Wales and S. West England	61500
`Total		300k
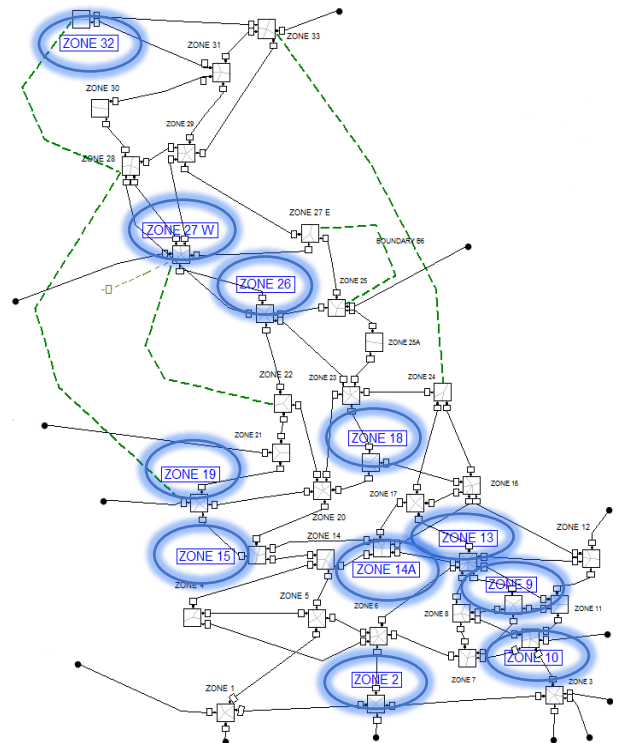
Fig. 9 Reduced GB 36-bus/substation transmission model
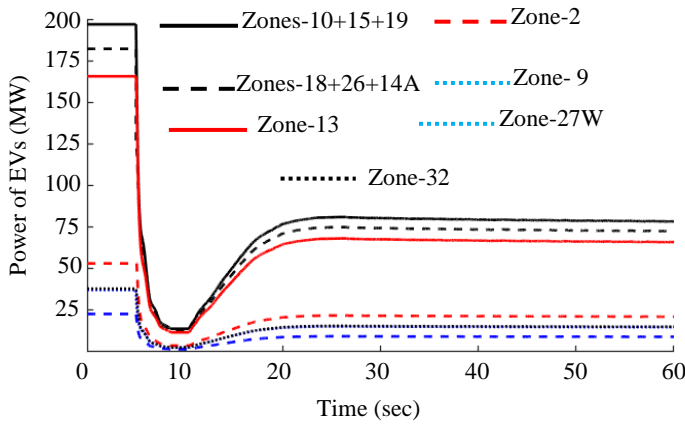
Fig.10 Power EVs at different zones
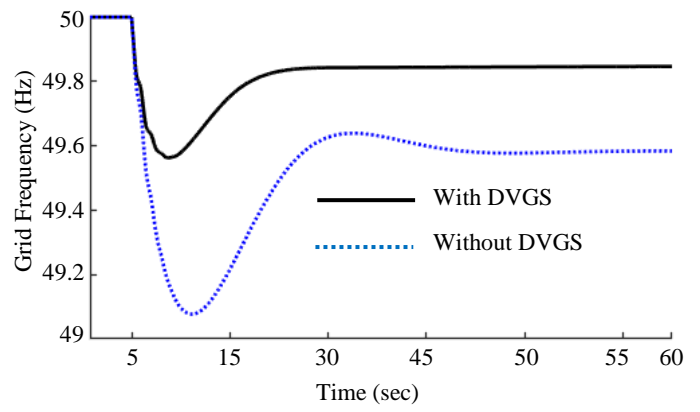
Fig.11 Variation of frequency after generation loss
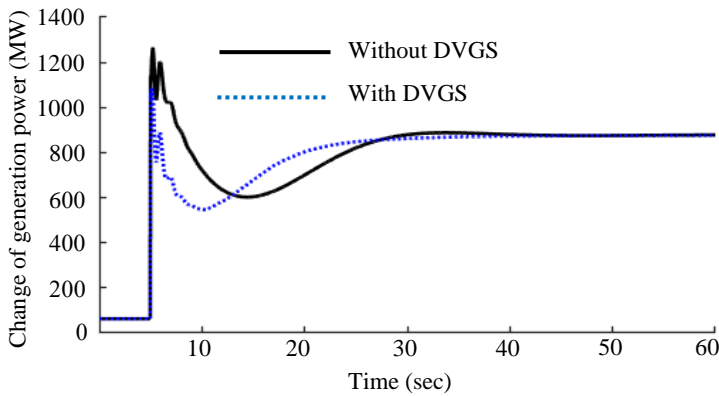
Fig.12 Change of power output (ΔP) of aggregated generators
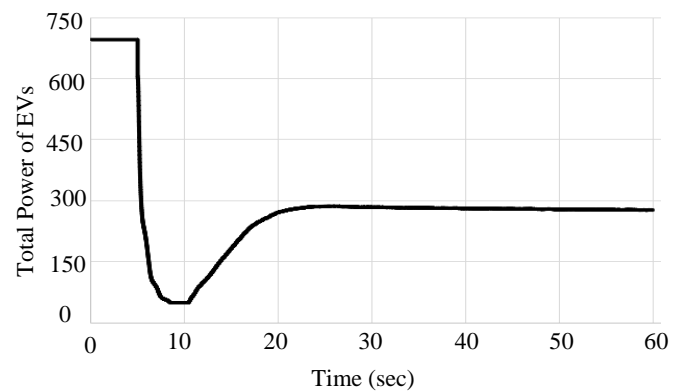
Fig.13 Power EVs at different zones

5.2 Case Study 2

This case study was conducted to investigate the effect of a population of DVGS control algorithms on the rate of change of frequency (RoCoF) during lagre imbalance contingencies applied to the GB reduced dynamic power system model. The RoCoF that would result from large frequency events ranging from 1 GW to 3 GW were envestigated, where the size and speed of the power change were very different. The National Grid aims to control the threshold level of RoCoF at an early stage following the incident, i.e., (0.5 sec) [29]. Figs. (14-17) show the RoCoF at early stages (i.e 0.05, 0.1, 0.2, and 0.5sec respectively) following the frequency events with and without the use of DVGS control algorithm. The frequency events were injected at time 1sec. Fig. 18 is the change of the charging power drwan by the EVs after using DVGS. We can see from Figs. (16-20) that a population of DVGS has reduced the RoCoF at the earliest sub-seconds follwing the imbalance contingencies. For example, with the 2GW loss of generation power, the RoCoF has decreased from 0.43mHz/sec to 0.4mHz/sec at time 1.05sec, from 0.77mHz/sec to 0.62mHz/sec at 1.1sec, from 1.15mHz/sec to 0.9mHz/sec at 1.2sec, and from from 0.85mHz/sec to 0.7mHz/sec at 1.5sec. The reduction of the RoCoF were obtained when the the DVGS reduced the charging power of the EVs by 20MW at time 1.05sec, 100MW at time 1.1sec, 450 at time 1.2sec, and 250MW at time 1.5sec (see Fig. 18 with frequency event 2GW). With the 3GW loss of generation power, around 600MW from the charging power was curtailed at time 0.5 follwing the frequency event by using 230k aggregated DVGS.
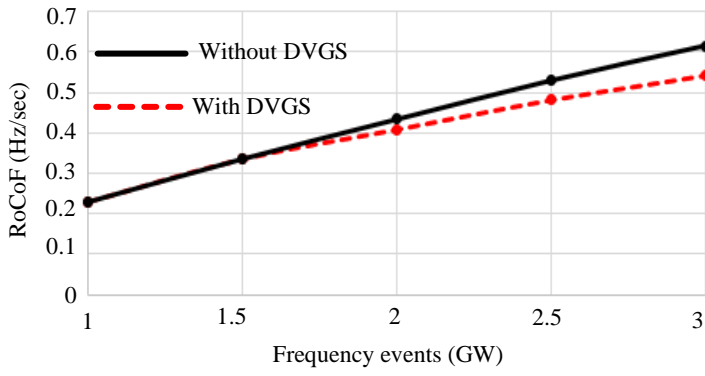
Fig. 14 Rate of change of frequency without DVGS model at 0.05sec following the event
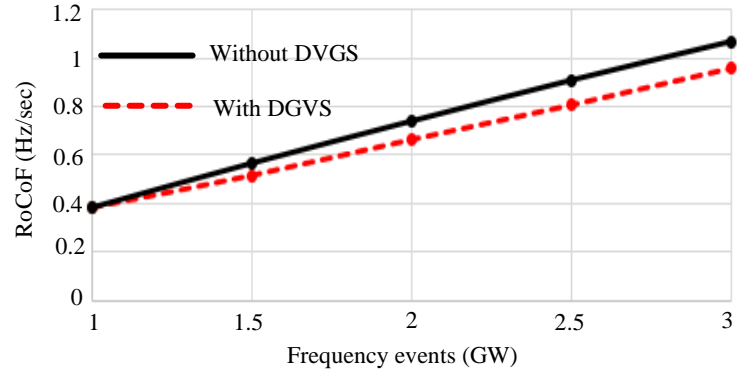
Fig. 15 Rate of change of frequency without DVGS model at 0.1sec following the event
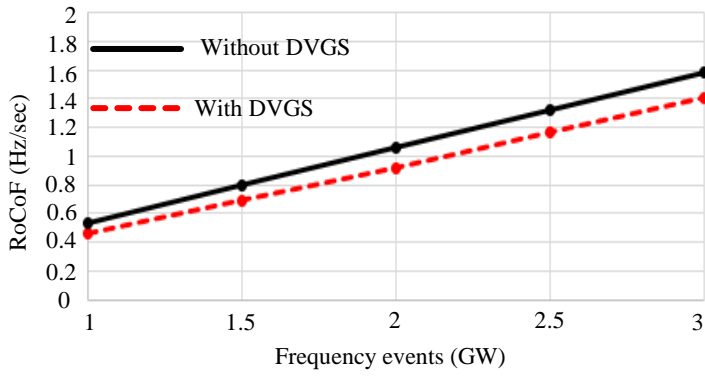
Fig. 16 Rate of change of frequency without DVGS model at 0.2sec following the event
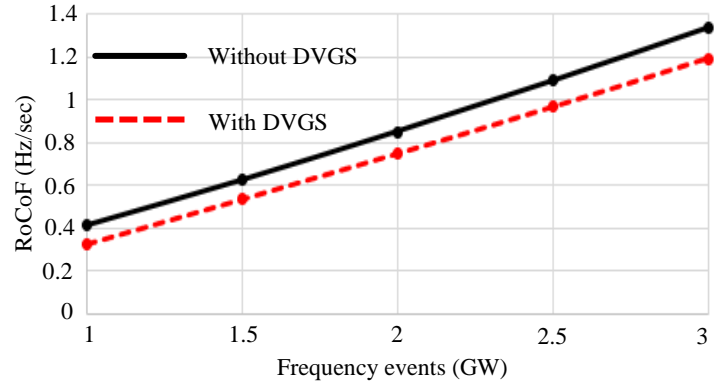
Fig. 17 Rate of change of frequency without DVGS model at 0.5sec following the event
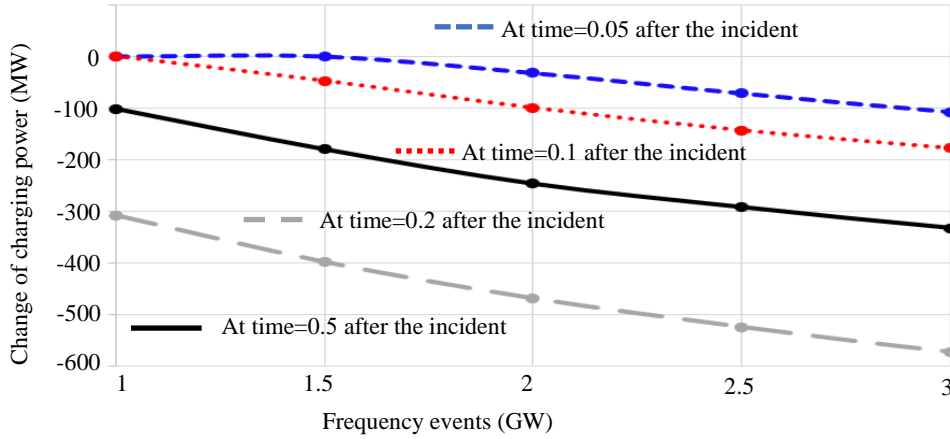
Fig. 18 Change of charging power drawn by EVs in response to frequency event

5.3 Financial Value of the aggregated DVGS

In this section, the financial benefits of using aggregated DVGS is briefly calculated. National Grid pays a total amount of £10.5 million for the total frequency response of 1,345,085 MWh every month through a FFR service [30]. We may observe that the total frequency response costs the UK £7.8/MWh per month. Then, the value of the aggregated DVGS (in £) to provide frequency response can be estimated using (8), where E_{res} in (£/MWh) is the total expenditure of the frequency response per MWh per month, P_{aggr}^{DVGS} in (MW) is the

volume of the frequency response provided by the aggregated DVGS, and t_{tend} in (hr) is the tendered time in which the DVGS is nominated to provide dynamic frequency response.

$$\text{Value } (£) = E_{res} \ (£/\text{MWh}) * \text{P}_{aggr}^{DVGS} \ (\text{MW}) * t_{tend} \tag{9}$$

It is assumed that the domestic EVs are plugged into the charging point after coming back home at time 18:00 and must be fully charged by 05:00, but can provide dynamic frequency response through that time. Giving that the maximum threshold time 7hr for each EV to be fully charged, the t_{tend} equal to 5hr (150 hour in a month). In this paper, a total frequenecy response of 650 MW was obtained by connecting 230k responsive EVs to the reduced GB power system (assuming that the power rate of each EV is 3kW for slow charging). Thus, using (9), the value of the aggregated 230k DVGS is £760,500/monthly (£9.125 million/yearly). The value contributed by each individual DVGS controller is £39.7 per year. However, the DVGS unit associated with each charging point is estimated to cost £10 (including the hardware and installation cost) [18]. Then, the net benefit from each DVGS unit is approximatly £29.7 per year.

However, this study considered only a slow charging scenario for domestic charging. For fast charging scenarios, the power rate of charging is higher (more than 6kW) which significantly increases the value of the frequency response contributed from each EV. Also, the above calculations neglected any value that could be earned from the reduction of greenhouse emissions (due to reduced part-loading).

6   Conclusion

This paper addressed the contribution of the frequency response ancillary services from the aggregation of residential EVs. A DVGS control algorithm was designed to control the behaviour of charging EV on the basis of a frequency signal. The DVGS controller has controlled the grid frequency by disconnecting the charging EVs according to the frequency signal. Frequency set-points were presented to vary dynamically with the state of charge of EVs. Charging controller during the critical time was added to the DVGS to ensure that the user will receive his/her EV fully charged in the morning regardless the frequency event.

The population of responsive EVs driven by the DVGS controllers were connected to the multi-zone reduced GB transmission power system model, with the predicted low inertia. The DVGS controllers distributed over the GB zones achieved an instantaneous zonal frequency response. The presented control algorithm helped to reduce the dependency on the frequency response provided by the conventional generators. Also, the load payback that could result from simultaneous reconnecting of EVs to the charging process is avoided as shown in Fig. 13. The finacial benefits of using aggregated DVGS to provide dynamic frequency respose was estimated.

The DVGS is a useful method to participate in providing a dynamic FFR service to the GB power system for the following reasons: I) The aggregation of EVs using the DVGS control method can provide, in each zone, the frequency response threshold of 1 MW, which is specified by National Grid to participate in the FFR service [31]. II) The DVGS control algorithm can alter the power consumption of EVs continuously to manage the second-by-second changes in the grid frequency.

Nevertheless, there were around 84k EVs have not provided frequency response because they reached fully charged before the occurance of the frequency event. There are some important measures that can be taken to address this issue. Firstly, smart charging scenario can be considered to ensure that the domestic EVs will not be fully charge by the time defined by the operator. Secondly, Vehicle to grid (V2G) technology is an important solution that can be used discharge the EVs back to the grid to provide low frequency response when the EVs reach fully charge. However, comprehensive studies are required to address the technical benefits of the combination of V2G technology with the DVGS in comparison to the economic viability, impact on battery, and social acceptance.

Acknowledgements

Appendix

In this section, table 3 is conducted to include a comparative study with other relevant studies presented in the literature.

Table 3 Comparative study with other relevant studies

Reference	Assets	proposed method	Type of behavior	type of charging	Dynamic Critical charging algorithm	Control setup
Current Work	EV	DVGS	Dynamic relationship between frequency set-points and SoC	Suitable for dumb charging	Dynamic Critical charging algorithm	decentralized
Ref[19]	EV	PFR	EV control based on EV charging load using statistical analysis	Suitable for different charging type	No	decentralized
Ref [21]	EV	Dynamic EV FC	EV droop control	For dumb charging	Forced charge boundary	decentralized
Refs [22, 32]	EV	DFC	EV droop control	For dumb charging	No	decentralized
Ref [23]	EV	DDC	SoC is updated dynamically based on droop control	For dumb charging	No	decentralized
Ref [33]	EV	FRC	droop control	Not specified	No	Centralized/ Limited communication

PFR: Primary Frequency Response
FC: Frequency Control
DDC: Dynamic Demand Control
DFC: Dynamic Frequency Control
FRC: Frequency Regulation Control

References

[1] National Grid. "'Frequency response services', 2019." https://www.nationalgrideso.com/balancing-services/frequency-response-services. [Accessed: 01-Nov-2019] (accessed.

[2] UK National Grid, "Enhanced Frequency Control Capability (EFCC), Jun. 2018 [Online]." [Online]. Available: https://www.nationalgrideso.com/document/120151/download

[3] D. M. Greenwood, K. Y. Lim, C. Patsios, P. F. Lyons, Y. S. Lim, and P. C. Taylor, "Frequency response services designed for energy storage," *Applied Energy*, vol. 203, pp. 115-127, 2017/10/01/ 2017, doi: https://doi.org/10.1016/j.apenergy.2017.06.046.

[4] W. Guo and J. Yang, "Modeling and dynamic response control for primary frequency regulation of hydro-turbine governing system with surge tank," *Renewable Energy*, vol. 121, pp. 173-187, 2018/06/01/ 2018, doi: https://doi.org/10.1016/j.renene.2018.01.022.

[5] M. Cheng, J. Wu, S. J. Galsworthy, N. Gargov, W. H. Hung, and Y. Zhou, "Performance of industrial melting pots in the provision of dynamic frequency response in the Great Britain power system," *Applied Energy*, vol. 201, no. Supplement C, pp. 245-256, 2017, doi: https://doi.org/10.1016/j.apenergy.2016.12.014.

[6] M. Cheng *et al.*, "Power System Frequency Response From the Control of Bitumen Tanks," *IEEE Transactions on Power Systems*, vol. 31, no. 3, pp. 1769-1778, 2016, doi: 10.1109/TPWRS.2015.2440336.

[7] M. T. Muhssin, L. Cipcigan, N. Jenkins, S. Slater, M. Cheng, and Z. Obaid, "Dynamic Frequency Response from Controlled Domestic Heat Pumps," *IEEE Transactions on Power Systems*, vol. PP, no. 99, pp. 1-1, 2018, doi: 10.1109/TPWRS.2017.2789205.

[8] M. T. Muhssin, L. M. Cipcigan, N. Jenkins, M. Cheng, and Z. A. Obaid, "Potential of a Population of Domestic Heat Pumps to Provide Balancing Service," *Journal Tehnički vjesnik/Technical Gazette*, vol. 25, no. 4, pp. 709-717, 2018.

[9] M. T. Muhssin, L. M. Cipcigan, S. S. Sami, and Z. A. Obaid, "Potential of demand side response aggregation for the stabilization of the grids frequency," *Applied Energy*, vol. 220, pp. 643-656, 2018/06/15/ 2018, doi: https://doi.org/10.1016/j.apenergy.2018.03.115.

[10] A. D. Paola, V. Trovato, D. Angeli, and G. Strbac, "A Mean Field Game Approach for Distributed Control of Thermostatic Loads Acting in Simultaneous Energy-Frequency Response Markets," *IEEE Transactions on Smart Grid*, vol. 10, no. 6, pp. 5987-5999, 2019, doi: 10.1109/TSG.2019.2895247.

[11] B. P. Roberts and C. Sandberg, "The Role of Energy Storage in Development of Smart Grids," *Proceedings of the IEEE*, vol. 99, no. 6, pp. 1139-1144, 2011, doi: 10.1109/JPROC.2011.2116752.

[12] B. Römer, P. Reichhart, J. Kranz, and A. Picot, "The role of smart metering and decentralized electricity storage for smart grids: The importance of positive externalities," *Energy Policy*, vol. 50, pp. 486-495, 2012/11/01/ 2012, doi: https://doi.org/10.1016/j.enpol.2012.07.047.

[13] X. Luo, J. Wang, M. Dooner, and J. Clarke, "Overview of current development in electrical energy storage technologies and the application potential in power system operation," *Applied Energy*, vol. 137, pp. 511-536, 2015/01/01/ 2015, doi: https://doi.org/10.1016/j.apenergy.2014.09.081.

[14] S. S. Sami, C. Meng, and W. Jianzhong, "Modelling and control of multi-type grid-scale energy storage for power system frequency response," in *2016 IEEE 8th International Power Electronics and Motion Control Conference (IPEMC-ECCE Asia)*, 22-26 May 2016 2016, pp. 269-273, doi: 10.1109/IPEMC.2016.7512297.

[15] M. Cheng, S. S. Sami, and J. Wu, "Benefits of using virtual energy storage system for power system frequency response," *Applied Energy*, vol. 194, no. Supplement C, pp. 376-385, doi: http://dx.doi.org/10.1016/j.apenergy.2016.06.113.

[16] Z. A. Obaid, L. M. Cipcigan, M. T. Muhssin, and S. S. Sami, "Control of a population of battery energy storage systems for frequency response," *International Journal of Electrical Power & Energy Systems*, vol. 115, p. 105463, 2020/02/01/ 2020, doi: https://doi.org/10.1016/j.ijepes.2019.105463.

[17] Z. A. Obaid, L. Cipcigan, and M. T. Muhssin, "Design of a hybrid fuzzy/Markov chain-based hierarchal demand-side frequency control," in *2017 IEEE Power & Energy Society General Meeting*, 16-20 July 2017 2017, pp. 1-5, doi: 10.1109/PESGM.2017.8273821.

[18] Element Energy, ""Frequency Sensitive Electric Vehicle and Heat Pump Power Consumption, final report for National Grid", July. 2015 ".

[19] Y. Mu, J. Wu, J. Ekanayake, N. Jenkins, and H. Jia, "Primary Frequency Response From Electric Vehicles in the Great Britain Power System," *IEEE Transactions on Smart Grid*, vol. 4, no. 2, pp. 1142-1150, 2013, doi: 10.1109/TSG.2012.2220867.

[20] L. Gong, W. Cao, K. Liu, Y. Yu, and J. Zhao, "Demand responsive charging strategy of electric vehicles to mitigate the volatility of renewable energy sources," *Renewable Energy*, 2020/04/18/ 2020, doi: https://doi.org/10.1016/j.renene.2020.04.061.

[21] J. Meng, Y. Mu, H. Jia, J. Wu, X. Yu, and B. Qu, "Dynamic frequency response from electric vehicles considering travelling behavior in the Great Britain power system," *Applied Energy*, vol. 162, pp. 966-979, 2016, doi: https://doi.org/10.1016/j.apenergy.2015.10.159.

[22] J. Meng, Y. Mu, J. Wu, H. Jia, Q. Dai, and X. Yu, "Dynamic frequency response from electric vehicles in the Great Britain power system," *Journal of Modern Power Systems and Clean Energy*, vol. 3, no. 2, pp. 203-211, 2015/06/01 2015, doi: 10.1007/s40565-015-0124-0.

[23] H. N. T. Nguyen, C. Zhang, and J. Zhang, "Dynamic Demand Control of Electric Vehicles to Support Power

Grid With High Penetration Level of Renewable Energy," *IEEE Transactions on Transportation Electrification,* vol. 2, no. 1, pp. 66-75, 2016, doi: 10.1109/TTE.2016.2519821.

[24]   M. Wang, Y. Mu, H. Jia, J. Wu, X. Yu, and Y. Qi, "Active power regulation for large-scale wind farms through an efficient power plant model of electric vehicles," *Applied Energy,* vol. 185, pp. 1673-1683, 2017/01/01/ 2017, doi: https://doi.org/10.1016/j.apenergy.2016.02.008.

[25]   J. Argueta and J. Smith, "Performance Characterization-1999 Nissan Altra-EV with Lithium-ion Battery, Sept, 1999 [Online]

".   [Online].   Available: file:///E:/My%20PhD/Old%20files%20related%20to%20my%20PhD/demand%20response/Casual%20work/ EV/EVs/altra_report.pdf

[26]   A.   Mendoza   and   J.   Argueta,   "Panasonic   Lead   Acid   Battery."   [Online].   Available: https://avt.inl.gov/sites/default/files/pdf/fsev/2000panpbaev1report.pdf

[27]   R. Ierna, J. Zhu, A. J. Roscoe, M. Yu, and A. Dysko, "Effects of VSM Convertor Control on Penetration Limits of Non-Synchronous Generation in the GB Power System " presented at the 15th Wind Integration Workshop, Vienna, Austria, 15 Nov 2016.

[28]   DCLG, "Table 401: Household projections," Department for Communities and Local Government. , 2016.

[29]   National Grid, "Frequency changes during large disturbances and their Impact on the Total System," National Grid. , Aug. 2013.

[30]   National Grid ESO, ""Monthly Balancing Services Summary," October, 2018 [Online]." [Online]. Available: https://www.nationalgrideso.com/document/133876/download

[31]   National Grid, "Demand Side Flexibility Annual Report 2017. Feb 2018, [Online]." [Online]. Available: http://powerresponsive.com/wp-content/uploads/2018/02/Power-Responsive-Annual-Report-2017.pdf

[32]   P. M. R. Almeida, F. J. Soares, and J. A. P. Lopes, "Electric vehicles contribution for frequency control with inertial emulation," *Electric Power Systems Research,* vol. 127, pp. 141-150, 2015/10/01/ 2015, doi: https://doi.org/10.1016/j.epsr.2015.05.026.

[33]   H. Yang, C. Y. Chung, and J. Zhao, "Application of plug-in electric vehicles to frequency regulation based on distributed signal acquisition via limited communication," *IEEE Transactions on Power Systems,* vol. 28, no. 2, pp. 1017-1026, 2013, doi: 10.1109/TPWRS.2012.2209902.